Box Splines

Hartmut Prautzsch, Wolfgang Boehm

This chapter provides a brief introduction to box and half-box splines with particular focus on triangular splines and surface design. A particular example of box splines are the B-splines with equidistant knots. In general, box splines consist of regularly arranged polynomial pieces and they have useful a geometric interpretation. Namely they can be viewed as density functions of the shadows of higher dimensional boxes and half-boxes. Of particular interest for Geometric Design are box spline surfaces that consist of triangular polynomial pieces. These box spline surfaces have planar domains, but it is quite simple to construct arbitrary two-dimensional surfaces, i.e, manifolds, with these box splines.

1. Box Splines

A very comprehensive treatment of box splines and their general theory is given in the book by de Boor, Höllig and Riemenschneider [10] who also give valuable information on many references.

1.1. Inductive Definition

An s-variate **box spline** $B(\mathbf{x}|\mathbf{v}_1 \dots \mathbf{v}_k)$ is determined by some k directions $\mathbf{v}_i$ in $\mathbb{R}^s$. For simplicity we will assume that $k \geq s$ and that $\mathbf{v}_1, \dots, \mathbf{v}_s$ are linearly independent. Under these assumptions the box splines $B_\kappa(\mathbf{x}) := B(\mathbf{x}|\mathbf{v}_1 \dots \mathbf{v}_\kappa), \kappa = s+1, \dots, k$, are defined by successive convolutions [21,22,35,6],

$$\begin{aligned} B_s(\mathbf{x}) &:= \begin{cases} 1/\det[\mathbf{v}_1 \dots \mathbf{v}_s] & \text{if} \quad \mathbf{x} \in [\mathbf{v}_1 \dots \mathbf{v}_s][0,1)^s \\ 0 & \text{else} \end{cases} \\ B_\kappa(\mathbf{x}) &:= \int_0^1 B_{\kappa-1}(\mathbf{x} - t\mathbf{v}_\kappa)dt, \quad \kappa > s \ . \end{aligned}$$

This is illustrated in Figure 1 for $s = 2$ and $[\mathbf{v}_1 \dots \mathbf{v}_4] = \begin{bmatrix} 1 & 0 & 1 & 1 \\ 0 & 1 & 1 & 0 \end{bmatrix}$. Figure 2 shows translates of some box splines that are tensor product box splines.

These box splines are normalized such that

$$\int_{\mathbb{R}^s} B_k(\mathbf{x})dx = 1 \ ,$$

which can easily be verified for $k = s$ and further by induction over k. Namely

$$\int_{\mathbb{R}^s} \int_0^1 B_{k-1}(\mathbf{x} - t\mathbf{v}_k)dtd\mathbf{x} = \int_0^1 \int_{\mathbb{R}^s} B_{k-1}(\mathbf{x} - t\mathbf{v}_k)d\mathbf{x}dt = \int_0^1 dt = 1 \ .$$

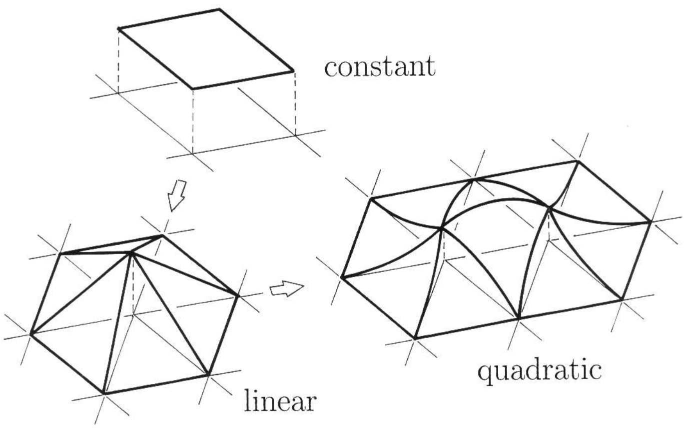

Figure 1. Bivariate box splines over the triangular grid.

1.2. Geometric Definition

A box spline $B_k(\mathbf{x}) = B(\mathbf{x}|\mathbf{v}_1 \ldots \mathbf{v}_k)$ can also be constructed geometrically. Namely it represents the density of the "shadow" of the unit cube $[0,1)^k$ under the affine map

$$\Phi(\mathbf{t}) = [\mathbf{v}_1 \ldots \mathbf{v}_k]\mathbf{t}$$

from $\mathbb{R}^k$ onto $\mathbb{R}^s$ as illustrated in Figure 3 for $k = 4$ and $s = 2$. This means

$$B_k(\mathbf{x}) = \mathrm{vol}_{k-s} C_k(\mathbf{x}) / |\det[\mathbf{v}_1 \ldots \mathbf{v}_s]| \ ,$$

where

$$\begin{aligned} C_k(\mathbf{x}) &:= \{\mathbf{t} \in [0,1)^k \mid [\mathbf{v}_1 \ldots \mathbf{v}_k]\mathbf{t} = \mathbf{x}\} \\ &= \Phi^{-}\mathbf{x} \cap [0,1)^k \ . \end{aligned}$$

For $k = s$ this fact is obvious and for greater k it follows by induction over k. Namely, $\sum_{i=1}^{k} t_i \mathbf{v}_i = \mathbf{x}$ if and only if $\sum_{i=1}^{k-1} t_i \mathbf{v}_i = \mathbf{x} - t_k \mathbf{v}_k$. Hence

$$\mathrm{vol}_{k-s} C_k(\mathbf{x}) = \int_0^1 \mathrm{vol}_{k-1-s} C_{k-1}(\mathbf{x} - t\mathbf{v}_k) dt \ ,$$

which corresponds to the inductive definition of the box splines and completes the proof.

Furthermore, the sets $C_k(\mathbf{x})$ are parallel for different $\mathbf{x}$. Therefore any regular affine map Ψ on $\mathbb{R}^k$ changes the volumes by a common factor. Thus, there is a constant γ such that

$$B_k(\mathbf{x}) = \gamma \cdot \mathrm{vol}_{k-s}(\Psi^{-1}\Phi^{-}\mathbf{x} \cap \Psi^{-1}[0,1)^k) \ .$$

The affine image $\beta = \Psi^{-1}[0,1)^k$ of the unit cube is called a **box** or a **parallelelepiped**. Hence the name box spline which is first used in [9].

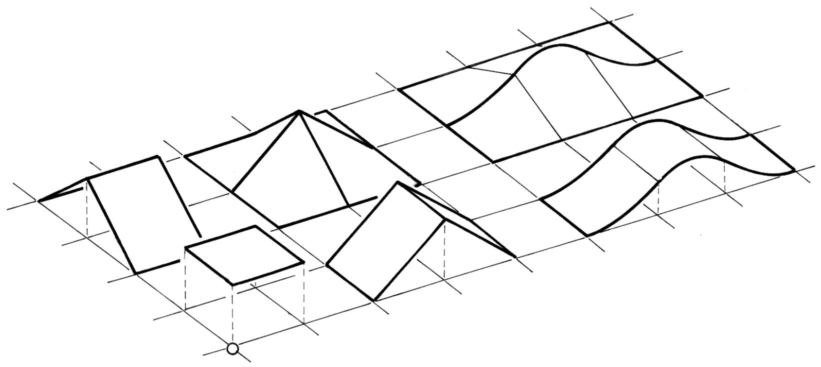

Figure 2. Translates of tensor product box splines.

In particular, if $\Pi := \Psi \circ \phi$ is the orthogonal projection

$$\Phi : [t_1 \ldots t_k]^t \mapsto [t_1 \ldots t_s]^t \quad ,$$

then $\gamma = \mathrm{vol}_k\beta$. Namely

$$\int_{\mathbb{R}^s} \mathrm{vol}_{k-s}(\Pi^{-}\mathbf{x} \cap \beta) d\mathbf{x} = \mathrm{vol}_k\beta \quad ,$$

which shows that

$$B_k(\mathbf{x}) = \mathrm{vol}_{k-s}(\Pi^{-}\mathbf{x} \cap \beta)/\mathrm{vol}_k\beta \tag{1}$$

is the correctly normalized box spline. The underlying geometric construction is illustrated in Figure 4 for $k = 3$ and $s = 2$. It is due to [6], while the idea of polyhedral shadows can be traced back to [36] and [37].

1.3. Further Definitions of Box Splines

From the geometric definition it follows that a box spline is characterizable as the solution of the functional equation

$$\int_{\mathbb{R}^s} B(\mathbf{x}|\mathbf{v}_1 \ldots \mathbf{v}_k) f(\mathbf{x}) d\mathbf{x} = \int_{[0,1)^k} f([\mathbf{v}_1 \ldots \mathbf{v}_k]\mathbf{t}) d\mathbf{t}$$

for all continuous test functions $f(\mathbf{x})$.

Another possibility to define a box spline is the following recursion

$$\begin{aligned} B(\mathbf{x}|\mathbf{v}_1 \ldots \mathbf{v}_k) &= \frac{1}{k-s} \sum_{r=1}^{k} (\alpha_r B(\mathbf{x}|\mathbf{v}_1 \ldots \mathbf{v}_r^* \ldots \mathbf{v}_k) \\ &\quad + (1-\alpha_r) B(\mathbf{x} - \mathbf{v}_r|\mathbf{v}_1 \ldots \mathbf{v}_r^* \ldots \mathbf{v}_k)) \quad , \end{aligned}$$

where $\mathbf{x} = \sum_{r=1}^{k} \alpha_r \mathbf{v}_r$. This recursion is due to de Boor and Höllig [8]. A geometric proof can be found in [4] and numerical and algorithmic aspects are discussed in [2,13,7,25].

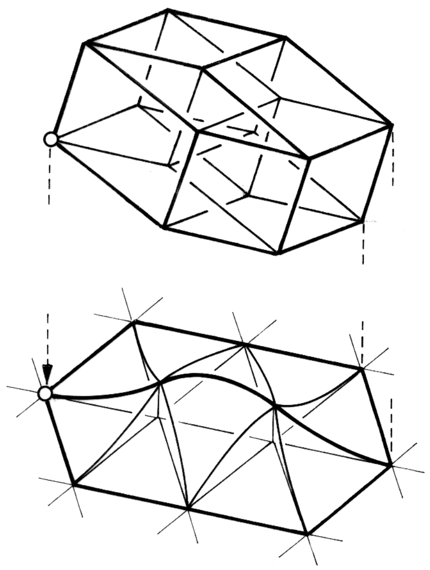

Figure 3. Box splines are "shadows" of boxes.

1.4. Basic Properties of Box Splines

From the geometric construction of box splines it follows that $B(\mathbf{x}) := B(\mathbf{x}|\mathbf{v}_1 \dots \mathbf{v}_k)$

- *does not depend on the* **ordering** *of the directions* $\mathbf{v}_i$,
- *is* **positive** *over the convex set* $[\mathbf{v}_1 \dots \mathbf{v}_k][0,1)^k$,
- *has the* **support** $suppB(\mathbf{x}) = [\mathbf{v}_1 \dots \mathbf{v}_k][0,1]^k$,
- *is* **symmetric** *with respect to the center of its support.*

Further, let $B(\mathbf{x})$ be the shadow of a box β as in (1). The $(s-1)$-dimensional faces of β projected into $\mathbb{R}^s$ form a tesselation of the support. It is illustrated in Figure 5 for

$$[\mathbf{v}_1 \dots \mathbf{v}_k] = \begin{bmatrix} 1 & 1 & 1 & 0 \\ -1 & 0 & 1 & 1 \end{bmatrix} \quad \text{and} \quad [\mathbf{v}_1 \dots \mathbf{v}_k] = \begin{bmatrix} 1 & 1 & 1 & 1 & 0 \\ 0 & 0 & 1 & 1 & 1 \end{bmatrix} .$$

- *The box spline* $B(\mathbf{x})$ *is polynomial of degree* $\leq k-s$ *over each tile of this partition.*

For a proof we observe that the extreme points of the convex sets $\pi^{-}\mathbf{x} \cap \beta$ lie in s-dimensional faces of β. Hence an extreme point is of the form $[\mathbf{x}^t\mathbf{e}^t]^t$, where $\mathbf{e} \in \mathbb{R}^{k-s}$ depends linearly on $\mathbf{x}$ over the projection of the corresponding s-dimensional face. The volume of $\pi^{-}\mathbf{x} \cap \beta$ can be expressed as a linear combination of determinants of $k-s \times k-s$ matrices whose columns represent differences of extreme points $\mathbf{e}$. Hence the volume is a polynomial of degree $\leq k-s$ in $\mathbf{x}$ over each tile of the tesselation above.

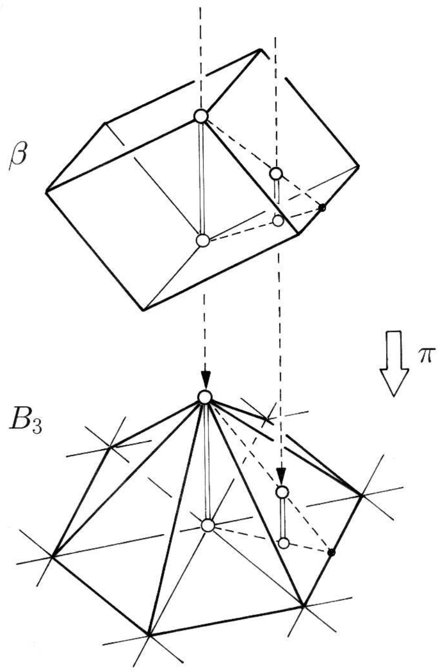

Figure 4. The geometric construction of a piecewise linear box spline over a triangular grid.

1.5. Derivatives

From the inductive or geometric definition it follows that the restricted box spline $B(y) := B(\mathbf{x} + y\mathbf{v}_r)$ is piecewise constant in y if $\mathbf{v}_r \notin \mathrm{span}\{\mathbf{v}_1, \ldots, \mathbf{v}_r^*, \ldots, \mathbf{v}_k\}$. If $\mathbf{v}_r \in \mathrm{span}\{\mathbf{v}_1, \ldots, \mathbf{v}_r^*, \ldots, \mathbf{v}_k\}$, then $B(y)$ is continuous since it can be obtained by a convolution from $B^*(y) = B(\mathbf{x} + y\mathbf{v}_r | \mathbf{v}_1 \ldots \mathbf{v}_r^* \ldots \mathbf{v}_k)$,

$$\begin{aligned} B(y) &= \int_0^1 B^*(y-t)dt = \int_{y-1}^{y} B^*(t)dt \\ &= \int_{-\infty}^{y} B^*(t) - B^*(t-1)dt \ . \end{aligned} \tag{2}$$

Further, the **directional derivative** with respect to $\mathbf{v}_r$ is given by

$$D_{\mathbf{v}_r} B(\mathbf{x}) = B'(y)|_{y=0} = B^*(\mathbf{x}) - B^*(\mathbf{x} - \mathbf{v}_r) \ . \tag{3}$$

If $\mathbf{v}_1, \ldots, \mathbf{v}_r^*, \ldots, \mathbf{v}_k$ span $\mathbb{R}^s$ for $r = 1, \ldots, s$, then $B(\mathbf{x})$ is continuous and its directional derivatives can be written as linear combinations of translates of the box splines $B(\mathbf{x}|\mathbf{v}_1 \ldots \mathbf{v}_r^* \ldots \mathbf{v}_k)$. Applying this argument repeatedly we see that

- *$B(\mathbf{x})$ is r times continuously differentiable if all subsets of $\{\mathbf{v}_1 \ldots \mathbf{v}_k\}$ obtained by deleting $r+1$ vectors $\mathbf{v}_i$ span $\mathbb{R}^s$.*

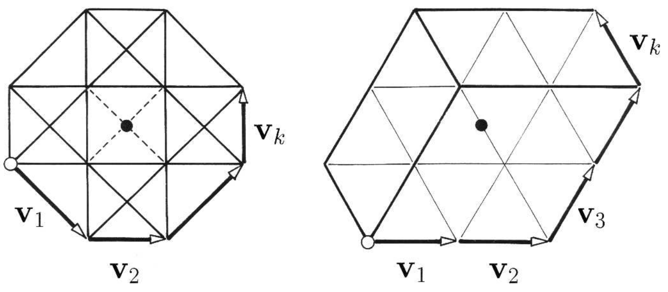

Figure 5. The supports of a quadratic and a cubic box spline over the criss cross and the regular triangular grid.

Remark: Another and inductive proof of the polynomial properties of $B(\mathbf{x})$ is based on (3). Namely, if $B^*(\mathbf{x})$ is a polynomial of degree $\leq k-s-1$ over each tile of the partition above, then $B^*(\mathbf{x}-\mathbf{v}_r)$ has the same property. Consequently $B(\mathbf{x})$ is piecewise polynomial of degree $k-s$ in each direction $\mathbf{v}_r$ over the partition above and hence in $\mathbf{x}$.

Remark: The piecewise quadratic C^1 box spline whose support is shown on the left side of Figure 5 is called a **Zwart-Powell element**. Because of its symmetry it is even quadratic and not piecewise quadratic over the inner square.

2. Box Spline Surfaces

2.1. Translates of Box Splines

In the sequel we assume that the directions $\mathbf{v}_1, \ldots, \mathbf{v}_k$ are in $\mathbb{Z}^s$ and, as before, that $\mathbf{v}_1, \ldots, \mathbf{v}_s$ span $\mathbb{R}^s$.

Obviously, the translates $B(\mathbf{x}-\mathbf{j}|\mathbf{v}_1 \ldots \mathbf{v}_s)$, $\mathbf{j} \in [\mathbf{v}_1 \ldots \mathbf{v}_s]\mathbb{Z}^s$, of the piecewise constant box spline sum to

$$\gamma := 1/|\det[\mathbf{v}_1 \ldots \mathbf{v}_s]| \ . \tag{4}$$

Since $\mathbb{Z}^s$ can be decomposed into, say m, sets $\mathbf{i} + [\mathbf{v}_1 \ldots \mathbf{v}_s]\mathbb{Z}^s$, see Figure 6, it follows that

$$\sum_{\mathbf{i}\in\mathbb{Z}^s} B(\mathbf{x}-\mathbf{i}|\mathbf{v}_1 \ldots \mathbf{v}_s) = m\gamma \ .$$

Further, since $\int_0^1 m\gamma dt = m\gamma$, we get by $k-s$ and again s successive convolutions

$$\begin{aligned} m\gamma &= \sum_{\mathbf{i}\in\mathbb{Z}^s} B(\mathbf{x}-\mathbf{i}|\mathbf{v}_1 \ldots \mathbf{v}_k) \\ &= \sum_{\mathbf{i}\in\mathbb{Z}^s} B(\mathbf{x}-\mathbf{i}|\mathbf{e}_1 \ldots \mathbf{e}_s\, \mathbf{v}_1 \ldots \mathbf{v}_k) \ , \end{aligned}$$

where $\mathbf{e}_i$ is the ith unit vector. Since the last sum is identically one due to (4), where $\mathbf{v}_1, \ldots, \mathbf{v}_k$ are replaced by $\mathbf{e}_1 \ldots \mathbf{e}_s$, we have shown that the (integer) shifts of any box spline $B(\mathbf{x}) := B(\mathbf{x}|\mathbf{v}_1 \ldots \mathbf{v}_k)$ form a **partition of unity**.

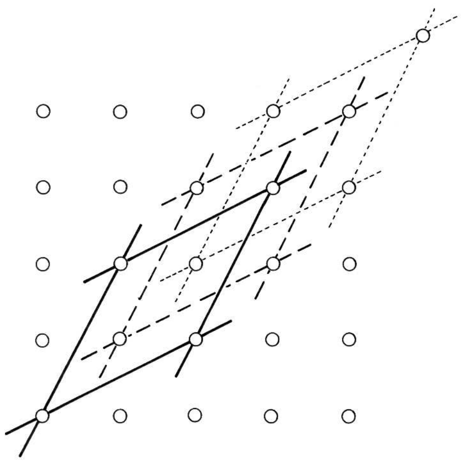

Figure 6. Decomposition of $\mathbb{Z}^s$ into translates of coarser grids.

Consequently, any **box spline surface**

$$\mathbf{s}(\mathbf{x}) = \sum_{\mathbf{i}\in\mathbb{Z}^s} \mathbf{c}_\mathbf{i} B(\mathbf{x}-\mathbf{i})$$

is an affine combination of its **control points** $\mathbf{c}_\mathbf{i}$ and this surface represenation is **affinely invariant** meaning that under any affine map the control point images control the surface image.

Since the box splines are non-negative, $\mathbf{s}(\mathbf{x})$ is even a convex combination of its control points and lies in their **convex hull**.

Further, we see that $B(\mathbf{x}-\mathbf{i}|\mathbf{v}_1 \dots \mathbf{v}_k), \mathbf{i} \in \mathbb{Z}^s$, is linearly dependent if $|\det[\mathbf{v}_1 \dots \mathbf{v}_s]| \neq 1$. Since the ordering of the $\mathbf{v}_i$ does not matter, this sequence is linearly dependent [9] also if there is any independent subsequence $\mathbf{v}_{i_1}, \dots, \mathbf{v}_{i_s}$ with $|\det[\mathbf{v}_{i_1} \dots \mathbf{v}_{i_s}]| \neq 1$. The converse is also true, see [16,19,23,24]. Together we have the following.

> $B(\mathbf{x}-\mathbf{i}|\mathbf{v}_1 \dots \mathbf{v}_k), \mathbf{i} \in \mathbb{Z}^s$, *is linearly independent over each open subset of* $\mathbb{R}^s$ *if and only if* $[\mathbf{v}_1 \dots \mathbf{v}_k]$ *is* **unimodular**,

which means that the determinant of any regular submatrix $[\mathbf{v}_{i_1} \dots \mathbf{v}_{i_s}]$ is 1 or -1.

2.2. Derivatives and Polynomial Properties

If the directions $\mathbf{v}_1, \dots, \mathbf{v}_{k-1}$ span $\mathbb{R}^s$, then we can compute the **directional derivative** $D_{\mathbf{v}_k}\mathbf{s}$ of $\mathbf{s}$ with respect to $\mathbf{v}_k$. Using the derivative formula (3) in 1.5 we obtain

$$D_{\mathbf{v}_k}\mathbf{s}(\mathbf{x}) = \sum_{\mathbf{i}\in\mathbb{Z}^s} \nabla_{\mathbf{v}_k}\mathbf{c}_\mathbf{i} B(\mathbf{x}-\mathbf{i}|\mathbf{v}_1 \dots \mathbf{v}_{k-1}) \ , \tag{5}$$

where $\nabla_\mathbf{v}\mathbf{c}_\mathbf{i} := \mathbf{c}_\mathbf{i} - \mathbf{c}_{\mathbf{i}-\mathbf{v}}$, see [9]. Further, if for all $j = 1, \dots, k$ the $k-1$ directions $\mathbf{v}_1, \dots, \mathbf{v}_j^* \dots \mathbf{v}_k$ span $\mathbb{R}^s$, then $B(\mathbf{x})$ is continuous as shown in 1.5 and the span of its shifts contains all linear polynomials as we show in the sequel. In particular, if

$$\mathbf{m_i} := \mathbf{i} + \frac{1}{2}(\mathbf{v}_1 + \cdots + \mathbf{v}_k)$$

denotes the **center** of supp$B(\mathbf{x} - \mathbf{i})$, then

$$\sum_{\mathbf{i} \in \mathbb{Z}^s} \mathbf{m_i} B(\mathbf{x} - \mathbf{i}) = \mathbf{x} \ . \tag{6}$$

Namely, because of symmetry, this equation holds for $\mathbf{x} = \mathbf{o}$ and for all $j = 1, \ldots, s$ we have [30]

$$D_{\mathbf{v}_j} \sum \mathbf{m_i} B(\mathbf{x} - \mathbf{i}) = \mathbf{v}_j \ .$$

Since the box spline representation is affinely invariant, we obtain for any linear polynomial $l(\mathbf{x})$

$$l(\mathbf{x}) = \sum l(\mathbf{m_i}) B(\mathbf{x} - \mathbf{i}) \ .$$

This property is referred to as the **linear precision** of the box spline representation.

More generally, let the directions $\mathbf{v}_1, \ldots, \mathbf{v}_k \in \mathbb{Z}^s$ span $\mathbb{R}^s$, and assume that the associated box spline $B(\mathbf{x}) := B(\mathbf{x}|\mathbf{v}_1 \ldots \mathbf{v}_k)$ is r times continuously differentiable. Then it follows, for example by induction over k that the map $c(\mathbf{x}) \mapsto \sum c(\mathbf{i}) B(\mathbf{x} - \mathbf{i})$ is a regular linear map on the space of all polynomials of degree $\leq r + 1$. See [9] for further results.

2.3. Convexity

Let $\mathbf{e}_1, \ldots, \mathbf{e}_s$ denote the unit directions and let $\mathbf{e} = \mathbf{e}_1 + \ldots + \mathbf{e}_s$. Further, let

$$\mathbf{s}(\mathbf{x}) = \sum_{\mathbf{i} \in \mathbb{Z}^s} \mathbf{c_i} B(\mathbf{x} - \mathbf{i} | \mathbf{e}_1 \ldots \mathbf{e}_1 \ldots \mathbf{e}_s \ldots e_s \mathbf{e} \ldots \mathbf{e})$$

be a box spline surface with these directions. The piecewise linear box spline surface

$$\mathbf{c}(\mathbf{x}) = \sum_{\mathbf{i} \in \mathbb{Z}^s} \mathbf{c_i} B(\mathbf{x} - \mathbf{i} | \mathbf{e}_1 \ldots \mathbf{e}_s \mathbf{e})$$

is said to be the control net of the surface $\mathbf{s}(\mathbf{x})$.

If the control net $\mathbf{c}(\mathbf{x})$ is a scalar valued and convex, then the surface $\mathbf{s}(\mathbf{x})$ is also a convex function, see [20,31]. Furthermore, any control net of $\mathbf{s}(\mathbf{x})$ obtained under subdvision as described next is convex [31].

2.4. Subdivision

Any box $\beta = [\mathbf{u}_1 \ldots \mathbf{u}_k][0,1)^k$ in $\mathbb{R}^k$ can be partitioned into 2^k translates of the scaled box $\hat{\beta} = \beta/2$ spanned by the half directions $\hat{\mathbf{u}}_i = \mathbf{u}_i/2$, see Figure 7. Based on this observation Prautzsch [28] concluded in 1993 that the non-normalized "shadow" $M_\beta(\mathbf{x}) = \mathrm{vol}_{k-s}(\pi^- \mathbf{x} \cap \beta)$ of β under the projection $\pi : [t_1 \ldots t_k]^t \mapsto [t_1 \ldots t_s]^t$ can be written as a linear combination of translates of the scaled box spline $M_{\hat{\beta}}(\mathbf{x}) = 2^{s-k} M_\beta(2\mathbf{x})$. Consequently, if the projections $\mathbf{v}_i = \pi \mathbf{u}_i$ lie in $\mathbb{Z}^s$, then any box spline surface

$$\mathbf{s}(\mathbf{x}) = \sum_{\mathbf{i} \in \mathbb{Z}^s} \mathbf{c}_\mathbf{i}^1 B(\mathbf{x} - \mathbf{i})$$

with $B(\mathbf{x}) = B(\mathbf{x}|\mathbf{v}_1 \dots \mathbf{v}_k)$ has also a “finer” representation

$$\mathbf{s}(\mathbf{x}) \quad = \quad \sum_{\mathbf{i} \in \mathbb{Z}^s} \mathbf{c}_{\mathbf{i}}^2 B(2\mathbf{x} - \mathbf{i}) \ .$$

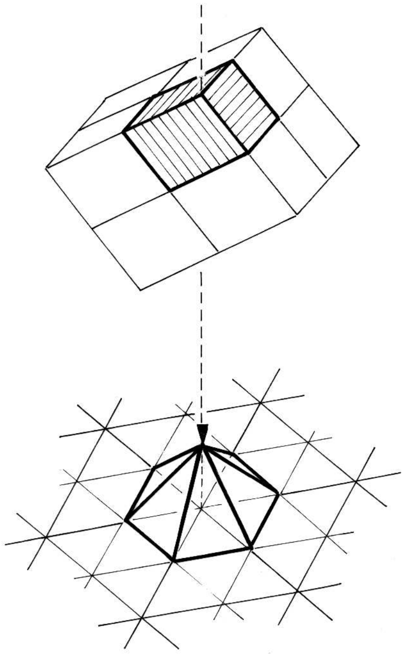

Figure 7. Subdividing a box spline by subdividing its box.

The new control points $\mathbf{c}_{\mathbf{i}}^2$ can be computed iteratively from the initial control points $\mathbf{c}_{\mathbf{i}}^1$ by the recursion

$$\begin{aligned}
\mathbf{d}^0(\mathbf{i}) \quad &:= \quad \begin{cases} \mathbf{o} & \text{if} \quad \mathbf{i}/2 \notin \mathbb{Z}^s \\ \mathbf{c}_{\mathbf{i}/2}^1 & \phantom{\text{if} \quad \mathbf{i}/2} \in \mathbb{Z}^s \end{cases} \ , \\
\mathbf{d}^r(\mathbf{i}) \quad &:= \quad (\mathbf{d}^{r-1}(\mathbf{j}) + \mathbf{d}^{r-1}(\mathbf{j} - \mathbf{v}_r))/2 \ , \quad r = 1 \dots k \ , \\
\mathbf{c}_{\mathbf{i}}^2 \quad &:= \quad 2^s \mathbf{d}^k(\mathbf{i}) \ .
\end{aligned}$$

For a proof we follow the ideas in [28] and subdivide each box $\beta_{r-1} = [\hat{\mathbf{u}}_1 \dots \hat{\mathbf{u}}_{r-1} \, \mathbf{u}_r \dots \mathbf{u}_k][0,1)^k$ into β_r and $\hat{\mathbf{u}}_r + \beta_r$. The associated shadows satisfy

$$M_{\beta_{r-1}}(\mathbf{x}) = M_{\beta_r}(\mathbf{x}) + M_{\beta_r}(\mathbf{x} - \hat{\mathbf{v}}_r) \ , \tag{7}$$

where $\hat{\mathbf{v}}_r = \mathbf{v}_r/2$. Dividing this equation by vol $\beta_{r-1} = 2\,\mathrm{vol}\beta_r$ gives

$$B_{r-1}(\mathbf{x}) = (B_r(\mathbf{x}) + B_r(\mathbf{x} - \hat{\mathbf{v}}_r))/2 \ , \tag{8}$$

where $B_r(\mathbf{x}) := B(\mathbf{x}|\hat{\mathbf{v}}_1 \ldots \hat{\mathbf{v}}_r \mathbf{v}_{r+1} \ldots \mathbf{v}_k)$.

Using this identity repeatedly and the relation $B(\mathbf{x}|\hat{\mathbf{v}}_1 \ldots \hat{\mathbf{v}}_k) = 2^s B(2\mathbf{x}|\mathbf{v}_1 \ldots \mathbf{v}_k)$ gives

$$\begin{aligned}
\mathbf{s}(\mathbf{x}) &= \sum_{\mathbf{i} \in Z^s} \mathbf{c}^1_{\mathbf{i}} B_0(\mathbf{x} - \mathbf{i}) \\
&= \sum_{\mathbf{i} \in Z^s} \mathbf{d}^r(\mathbf{i}) B_r(\mathbf{x} - \mathbf{i}/2) \ , \quad r = 0, 1 \ldots k \ , \\
&= \sum_{\mathbf{i} \in Z^s} \mathbf{c}^2_{\mathbf{i}} B_0(2\mathbf{x} - \mathbf{i}) \ ,
\end{aligned}$$

which concludes the proof.

For quadratic univariate box splines with equdistant knots this algorithm bears the name of Chaikin [11] although it had been discussed already by de Rham [34]. Lane and Riesenfeld [26] generalized Chaikin's algorithm to univariate box splines of arbitrary degree with equidistant knots and in [3], which prepublishes, results of [28] a mask is introduced to describe the subdivision algorithm above for three direction box splines. Later Loop [27] used Boehm's mask to build a subdivision algorithm for arbitrary triangular nets.

Remark: If $[\mathbf{v}_1 \ldots \mathbf{v}_s]Z^s = Z^s$, then $2^s \mathbf{d}^s_{\mathbf{i}} = \mathbf{c}^1_{\lfloor \mathbf{i}/2 \rfloor}$ and every point $\mathbf{c}^2_{\mathbf{i}}$ is a convex combination of the initial points $\mathbf{c}^1_{\mathbf{i}}$. Moreover, the $\mathbf{c}^2_{\mathbf{i}}$ lie in the convex hull of the $\mathbf{c}^1_{\mathbf{i}}$ also if $[\mathbf{v}_1 \ldots \mathbf{v}_s]Z^k = Z^s$.

2.5. General Subdivision

It is straightforward to generalize the subdivision algorithm to obtain for any $m \in \mathbb{N}$ the finer representation

$$\mathbf{s}(\mathbf{x}) = \sum_{\mathbf{i} \in Z^s} \mathbf{c}^m_{\mathbf{i}} B(m\mathbf{x} - \mathbf{i}) \ ,$$

where the "points" $\mathbf{c}^m_{\mathbf{i}} = m^s \mathbf{d}^k(\mathbf{i})$ can be computed successively by

$$\begin{aligned}
\mathbf{d}^0(\mathbf{i}) &:= \begin{cases} \mathbf{o} & \text{if } \ \mathbf{i}/m \notin Z^s \\ \mathbf{c}^1_{\mathbf{i}/m} & \text{if } \ \mathbf{i}/m \in Z^s \end{cases} \ , \\
\mathbf{d}^r(\mathbf{i}) &:= \frac{1}{m} \sum_{l=0}^{m-1} \mathbf{d}^{r-1}(\mathbf{i} - l\mathbf{v}_r) \ , \quad r = 1, \ldots, k \ .
\end{aligned}$$

In this and in an even more general form this algorithm can be found in [12] and [17,18], where it is derived algebraically.

The subdivision algorithm can be used a second time to compute control points of $\mathbf{s}(\mathbf{x})$ over any finer grid $Z^s/(mn)$. Since the partition of a box β into translates of the scaled box $\beta/(mn)$ is unique, we get as a result the same points $\mathbf{c}^{mn}_{\mathbf{i}}$ that can be computed directly from the initial control points $\mathbf{c}^1_{\mathbf{i}}$ by one application of the subdivision algorithm.

Similarly we see that the points $\mathbf{c}^m_{\mathbf{i}}$ do not depend on the ordering of the directions $\mathbf{v}_1, \ldots, \mathbf{v}_k$, i.e., the ordering of the averaging steps.

Remark: The geometric derivation of the subdivision algorithm above shows that any new control point $\mathbf{c}^m_{\mathbf{j}}$ only depends on the control points $\mathbf{c}^1_{\mathbf{i}}$, where $\operatorname{supp} B(m\mathbf{x} - \mathbf{j}) \subset$

$\operatorname{supp} B(\mathbf{x}-\mathbf{i})$. Their number is bounded by some h not depending on m and $\mathbf{j}$. Hence we have

$$\|\mathbf{c}_\mathbf{j}^m\| \leq h \sup_{\mathbf{i}\in \mathbb{Z}^s} \|\mathbf{c}_\mathbf{i}^1\| \ . \tag{9}$$

2.6. Convergence under subdivision

Repeated subdivision by the algorithm 2.5 gives the control points of the finer representation

$$\mathbf{s}(\mathbf{x}) = \sum_{\mathbf{i}\in \mathbb{Z}^s} \mathbf{c}_\mathbf{i}^m B(m\mathbf{x}-\mathbf{i}) \ , \quad \text{where} \quad B(\mathbf{x}) = B(\mathbf{x}|\mathbf{v}_1 \ldots \mathbf{v}_k) \ ,$$

of any surface $\mathbf{s}(\mathbf{x})$ over all scaled grids $\mathbb{Z}^s/m$, $m \in \mathbb{N}$. A major value of this procedure is that under some reasonable conditions on $V = [\mathbf{v}_1 \ldots \mathbf{v}_k]$ the points $\mathbf{c}_\mathbf{i}^m$ converge towards $\mathbf{s}(\mathbf{x})$, see [26,28,29,15,14].

Let h be as in (9) and $M = \sup\{||\nabla_{\mathbf{v}_r} \mathbf{c}_\mathbf{i}^1||$, where $\mathbf{i} \in \mathbb{Z}^s$ and $\mathbf{v}_1, \ldots, \mathbf{v}_r^*, \ldots, \mathbf{v}_k$ span $\mathbb{R}^s$. Then the following holds.

If $[\mathbf{v}_1 \ldots \mathbf{v}_k]\mathbb{Z}^k = \mathbb{Z}^s$, *then* $\|\mathbf{c}_\mathbf{i}^m - \mathbf{s}(\mathbf{x})\| \leq hM/m$ *for all* $\mathbf{i}$, *where* $B(m\mathbf{x}-\mathbf{i}) > 0$.

In this generality this result is due to de Boor et al. [10] who also show quadratic convergence under the conditions $[\mathbf{v}_1 \ldots \mathbf{v}_i^* \ldots \mathbf{v}_k]\mathbb{Z}^{k-1} = \mathbb{Z}^s$ and $B(\mathbf{x}|\mathbf{v}_1 \ldots \mathbf{v}_k)$ is differentiable.

On the other hand if $[\mathbf{v}_1 \ldots \mathbf{v}_k]\mathbb{Z}^k \neq \mathbb{Z}^s$, then convergence cannot be proved as we show for $s(\mathbf{x}) = B(\mathbf{x})$.

Namely, if there is some grid point $\mathbf{i} \in \mathbb{Z}^s$, which does not lie in $[\mathbf{v}_1 \ldots \mathbf{v}_k]\mathbb{Z}^k$, then all grid points $\mathbf{j} \in J := \mathbf{i} + [\mathbf{v}_1 \ldots \mathbf{v}_s]\mathbb{Z}^s$ do also not lie in $[\mathbf{v}_1 \ldots \mathbf{v}_k]\mathbb{Z}^k$. Since $\sum_{\mathbf{j}\in J} B(\mathbf{x}-\mathbf{j}) > 0$, see (4) in 2.1, there is for every $\mathbf{x} \in \mathbb{R}^s$ some $\mathbf{j} \in J$ such that $B(\mathbf{x}-\mathbf{j}) > 0$.

Subdividing the single box spline $B(\mathbf{x})$ by the algorithm in 2.5 gives control points $c_\mathbf{i}^m$ such that

$$B(\mathbf{x}) = \sum_{\mathbf{i}\in \mathbb{Z}^s} \mathbf{c}_\mathbf{i}^m B(m\mathbf{x}-\mathbf{i}) \ .$$

The geometric derivation of the algorithm in 2.4 shows that $\mathbf{c}_\mathbf{i}^m \neq 0$ if and only if $\mathbf{i} \in [\mathbf{v}_1 \ldots \mathbf{v}_k]\mathbb{Z}_m^k$.

Thus if $[\mathbf{v}_1 \ldots \mathbf{v}_k]\mathbb{Z}^k \neq \mathbb{Z}^s$ or $J \neq \emptyset$, there is for every $\mathbf{x} \in \mathbb{R}^s$ some zero control point $\mathbf{c}_\mathbf{j}^m = 0$ with $B(m\mathbf{x}-\mathbf{j}) > 0$. For all $\mathbf{x}$, where $B(\mathbf{x}) > 0$, these control points do not converge to $B(\mathbf{x})$ as m tends to infinity.

2.7. Bézier Representation

Often it is useful or neccessary to have the Bézier representation of a box spline surface. In this section we describe how to compute the Bézier points of a box spline surface over a regular triangular grid, see also [35,1,28,5].

Let $\mathbf{e}_1, \mathbf{e}_2, \mathbf{e}_3$ be the unit directions $[1\ 0]^t, [0\ 1]^t, -[1\ 1]^t$ and let $\mathbf{v}_1, \ldots, \mathbf{v}_k \in \{\mathbf{e}_1, \mathbf{e}_2, \mathbf{e}_3\}$. Further let $\mathbf{b}_n(\mathbf{i}), \mathbf{i} \in \mathbb{Z}^2$, be the Bézier points of the box spline surface

$$\mathbf{s}_n(\mathbf{x}) = \sum_{\mathbf{i}\in \mathbb{Z}^2} \mathbf{c}_\mathbf{i} B(\mathbf{x}-\mathbf{i}|\mathbf{e}_1\mathbf{e}_2\mathbf{v}_1 \ldots \mathbf{v}_n)$$

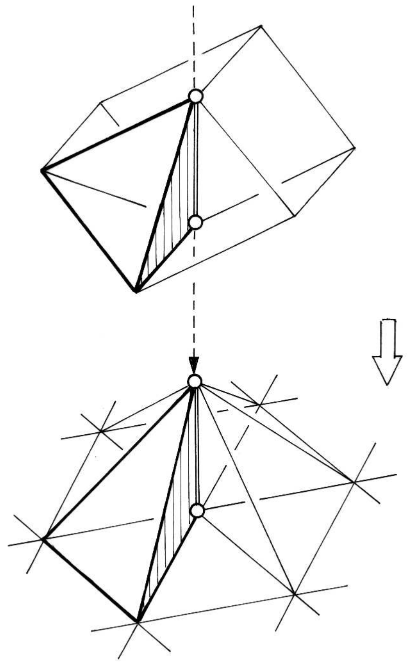

Figure 8. Bernstein polynomials are shadows of simplices.

such that $\mathbf{s}_n(\mathbf{x})$ restricted to some grid triangle with vertices $\mathbf{a}, \mathbf{a}+\mathbf{e}_1, \mathbf{a}-\mathbf{e}_\mu$ and $\mu = 2$ or 3 has the Bézier representation

$$\mathbf{s}_n(\mathbf{x}) = \sum \mathbf{b}_n(n\mathbf{a} + i\mathbf{e}_1 + j\mathbf{e}_\mu)\frac{n!}{i!j!k!}u^i v^j w^k \ ,$$

where $i + j + k = n$ and $\mathbf{x} = u\mathbf{a} + v(\mathbf{a}+\mathbf{e}_1) + w(\mathbf{a}-\mathbf{e}_\mu)$.

Recall that integration means summation of the Bézier points. Consequently, since

$$\mathbf{s}_n(\mathbf{x}) = \int_0^1 \mathbf{s}_{n-1}(\mathbf{x} - t\mathbf{v}_n)dt \ ,$$

we can compute the Bézier points $\mathbf{b}_n(\mathbf{i})$ recursively from the copies

$$\mathbf{a}_n(n\mathbf{j} + \mathbf{v}_n - r\mathbf{e}_\mu - s\mathbf{e}_\nu) := \mathbf{b}_{n-1}((n-1)\mathbf{j} - r\mathbf{e}_\mu - s\mathbf{e}_\nu) \ ,$$

where $\mu, \nu \in 1, 2, 3$ and $\mathbf{e}_\mu + \mathbf{e}_\nu = -\mathbf{v}_n$ and $r, s = 0, ..., n-1$ and $\mathbf{j} \in \mathbb{Z}^2$, by the summation

$$\mathbf{b}_n(\mathbf{i}) := \frac{1}{n}\sum_{\nu=0}^{n-1} \mathbf{a}(\mathbf{i} - \nu\mathbf{v}_n)$$

as is illustrated schematically in Figure 9 for $n = 3$.

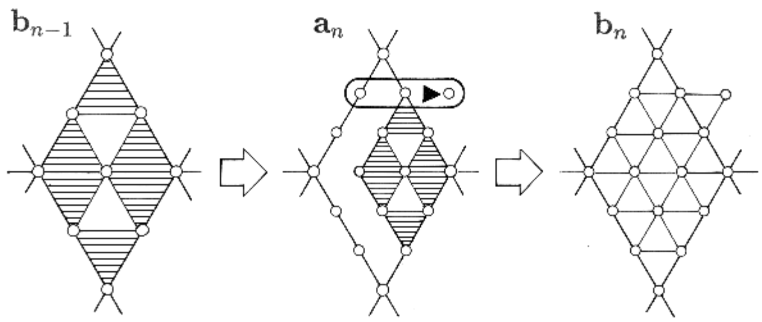

Figure 9. Computing Bézier points recursively.

If $\mathbf{v}_1 = \mathbf{e}_3$, then $\mathbf{b}_1(\mathbf{i}) = \mathbf{c}_\mathbf{i}$, which terminates the recursion.
Note that the Bézier net $\mathbf{b}_n$ can be computed faster if the summation is replaced by

$$\mathbf{b}_n(\mathbf{i}) := \mathbf{b}_n(\mathbf{i} - \mathbf{v}_n) + [\mathbf{a}_n(\mathbf{i}) - \mathbf{a}_n(\mathbf{i} - n\mathbf{v}_n)]/n \ .$$

The summation step can also be described by a convoulution of $\mathbf{a}_n$ with the mask

$$\sigma_n(\mathbf{i}) = \begin{cases} 1/n & \text{for} \quad \mathbf{i} = \mathbf{o}, -\mathbf{v}_n, \dots, -(n-1)\mathbf{v}_n \\ 0 & \text{otherwise} \end{cases}$$

defined on $\mathbb{Z}^2$. This means

$$\mathbf{b}_n = \mathbf{a}_n * \sigma_n \ ,$$

where

$$(\mathbf{a}_n * \sigma_n)(\mathbf{i}) = \sum_{\mathbf{j} \in \mathbb{Z}^2} \mathbf{a}_n(\mathbf{j}) \sigma_n(\mathbf{j} - \mathbf{i}) \ .$$

2.8. Bézier Representation of Symmetric Box Splines

Of particular interest are the symmetric box splines, where $\mathbf{e}_1\mathbf{e}_2\mathbf{v}_1 \dots \mathbf{v}_n = \mathbf{e}_1\mathbf{e}_2\mathbf{e}_3 \dots \mathbf{e}_1\mathbf{e}_2\mathbf{e}_3$. For these box splines there is a symmetric version of the algorithm above. Combining three successive integrations leads to the recursion

$$\mathbf{b}_n = C_n \mathbf{b}_{n-3} * \alpha_n \ ,$$

where the mask α_n represents a degree elevated Bézier net of the symmetric piecewise linear box spline,

$$\alpha(\mathbf{i}) = B(\mathbf{i}/n | \mathbf{e}_1\mathbf{e}_2\mathbf{e}_3) \ ,$$

and where $C_n\mathbf{b}_{n-3}$ is a copy with additionally zeroes of the Bézier net $\mathbf{b}_{n-3}$ as illustrated in Figure 10 for $n = 5$.

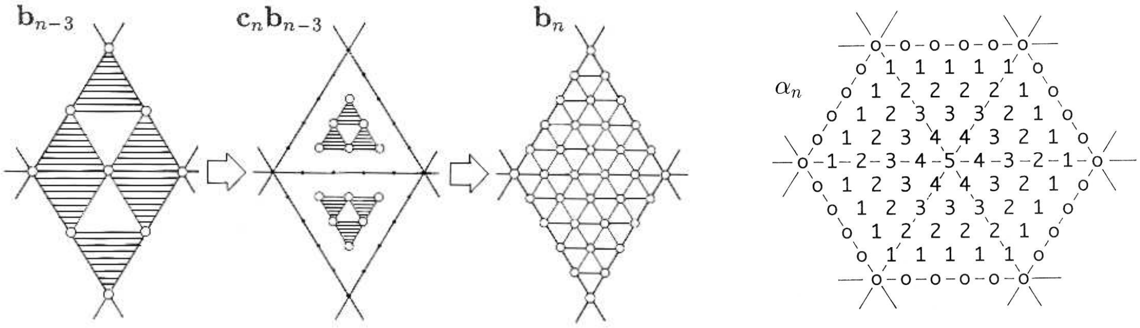

Figure 10. Symmetric recursion for the Bézier points.

Formally, C_n is defined by

$$C_n\mathbf{b}_{n-3}(n\mathbf{i}-(r+1)\mathbf{e}_1-(s+1)\mathbf{e}_\mu) = \begin{cases} \mathbf{o} & \text{for} \quad r \quad \text{or} \quad s=-1 \\ \mathbf{b}_{n-3}((n-3)\mathbf{i}+r\mathbf{e}_1-s\mathbf{e}_\mu) & \text{for} \quad r,s=0,\dots,n-3 \end{cases}$$

for $\mathbf{i} \in \mathbb{Z}^2$.

The computation of the Bézier points can be organized in different ways. In the sequel we present the geometrically nice one due to [1].

Let β be the Bézier net of the box spline $B(\mathbf{x}|\mathbf{e}_1\mathbf{e}_2\mathbf{v}_1\dots\mathbf{v}_n)$ and let $\gamma = C_n\beta$. Then

$$\begin{aligned} \mathbf{b}_n(\mathbf{j}) &= \sum_{\mathbf{i}\in\mathbb{Z}^2} \mathbf{c}_\mathbf{i}\beta(\mathbf{k}-\mathbf{i}) * \alpha(\mathbf{k}) \\ &= \sum_{\mathbf{k}}\sum_{\mathbf{i}} \mathbf{c}_\mathbf{i}\beta(\mathbf{k}-\mathbf{i}) \cdot \alpha(\mathbf{k}) \\ &= \sum_{\mathbf{l}}\sum_{\mathbf{i}} \mathbf{c}_\mathbf{i}\alpha(\mathbf{l}-\mathbf{i}) \cdot \beta(\mathbf{j}-\mathbf{l}) \\ &= \sum_{\mathbf{i}} \mathbf{c}_\mathbf{i}\alpha(\mathbf{l}-\mathbf{i}) * \beta(\mathbf{l}) \end{aligned}$$

The net $\sum_\mathbf{i} \mathbf{c}_\mathbf{i}\alpha(\mathbf{l}-\mathbf{i})$ is the Bézier net $\mathbf{b}_1$ after raising the degree from 1 to n. It is a refinement of the control net. Together with the mask $\beta(\mathbf{l})$ it is shown in Figure 11 for $n=4$.

2.9. Generalized Box Spline Surfaces

A bivariate box spline surface has a planar domain. However, with the symmetric box splines

$$B_k(\mathbf{x}) = B(\mathbf{x}|\mathbf{e}_1\mathbf{e}_2\mathbf{e}_3 \overset{k}{\dots} \mathbf{e}_1\mathbf{e}_2\mathbf{e}_3)$$

it is possible to build smooth arbitrarily free-form surfaces with non-planar domains. The support of the box splines $B_k(\mathbf{x})$ consists of k rings of triangles as shown in Figure 12 for

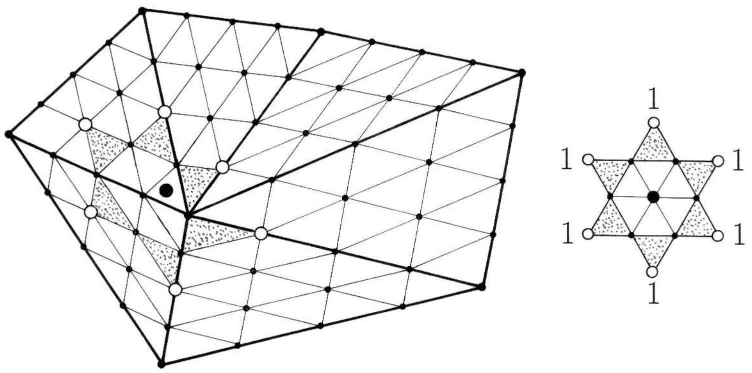

Figure 11. Computing the Bézier points of a quartic box spline surface.

$k = 2, 3$. This implies that any triangular patch of a box spline surface

$$\mathbf{s}(\mathbf{x}) = \sum_{\mathbf{i} \in \mathbb{Z}^2} \mathbf{c}_{\mathbf{i}} B_k(\mathbf{x})$$

is controlled by k rings of control points as illustrated schematically in Figure 13 for $k = 2, 3$.

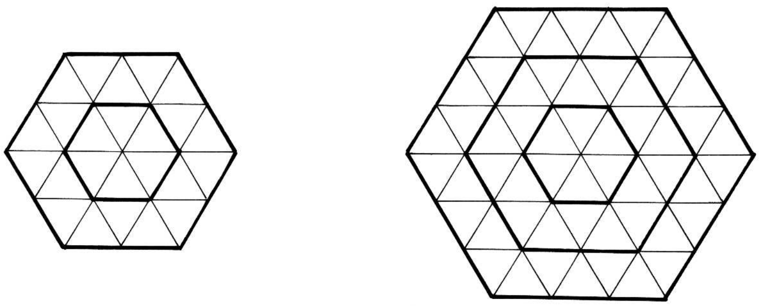

Figure 12. Support of the box splines B_2 (left) and B_3 (right).

We will call the net controlling one triangular patch a **minimal net** or a **B-primitive** of order k.

A **generalized box spline surface** of degree $3k - 2$ or order k is given by an arbitrary control net and consists of all triangular patches controlled by a B-primitive of order k that is part of the entire control net.

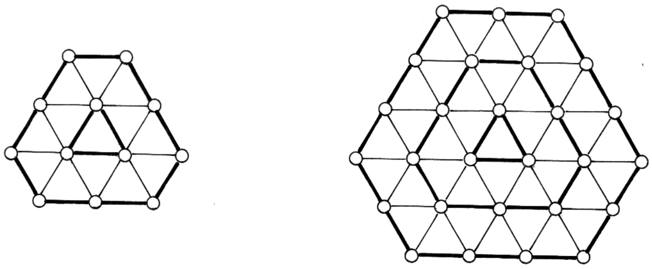

Figure 13. Net primitives of order 2 (left) and 3 (right).

An interior vertex of the triangular control net is called **regular** if it has valence 6 and otherwise it is called **irregular**. If the irregular vertices of a triangular net are surrounded by sufficiently many regular vertices, then the generalized box spline surface has an m-sided hole for any irregular vertex with valence m as illustrated schematically in Figure 14 for $k = 2$ and $m = 4$ with a generalized box spline surface consisting of 2 rings of triangular patches around a four sided hole. Such a hole can be filled smoothly by $k-1$ rings of triangles.

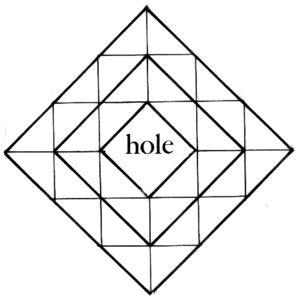

Figure 14. Schematic view of a hole of a generalized box spline surface of order 2.

The larger k, the larger the holes are schematically. A remedy for this is to let $k-2$ rings of control points around an irregular control point coalesce as illustrated schematically in Figure 15 for $k = 3$ and $m = 4$. When looking for the net primitives in the overall control net we interpret these multiple control points in different ways as part of a regular triangular net that is collapsed into this one point so as to obtain as many net primitives as possible. Thus, the schematic size of the holes depends only on m and is the same for all k.

These holes can be filled with m triangular patches of degree $2k$ with G^k-joints, see

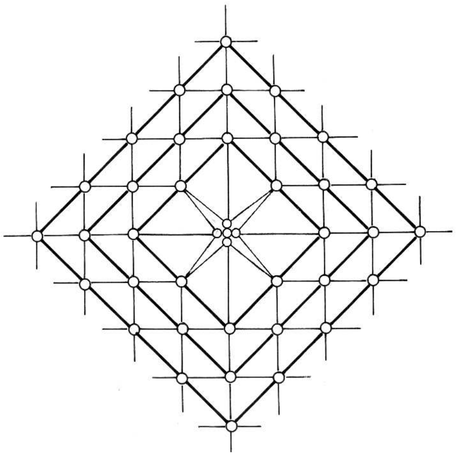

Figure 15. Control net of a generalized box spline surface of order 3 with multiple irregular vertex.

[38,32,33]. Figure 16 shows an example of a generalized box spline surface of order $k = 2$. The control net is seen left, the generalized box spline surface in the middle and on the right the holes are filled with octic polynomials so as to obtain an overall curvature continous surface.

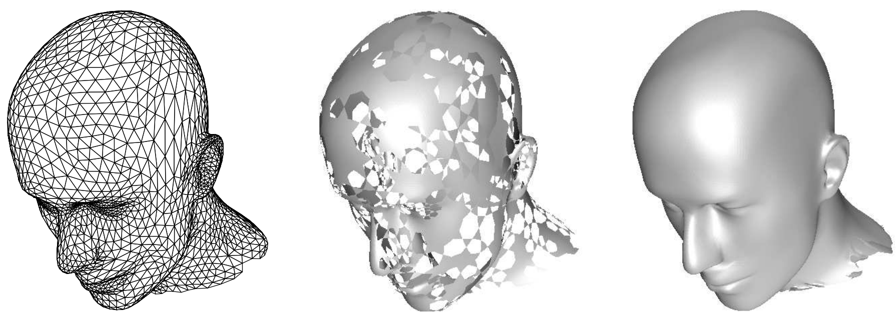

Figure 16. A generalized box spline surface of order 2 (middle) with control net (left) and G^2-fillings (right). (courtesy of Georg Umlauf)

3. Half-Box Splines

3.1. Inductive Definition

Half-box splines are defined over the triangular grid spanned by $\mathbf{e}_1 = [1\ 0]^t, \mathbf{e}_2 = [0\ 1]^t$ and $\mathbf{e}_3 = -[1\ 1]^t$. We give the inductive definition due to Sabin [35] and its geometric interpretation due to [28].

Splitting the unit square along its diagonal in direction $\mathbf{e}$ gives the two triangles

$$\Delta := \{\mathbf{x} | 0 \le x \le y < 1\} \quad \text{and} \quad \nabla := \{\mathbf{x} | 0 \le y < x < 1\} \ .$$

They support the piecewise constant half-box splines

$$H_\Delta(\mathbf{x}|) := \begin{cases} 1 & \text{if} \quad \mathbf{x} \in \Delta \\ 0 & \text{else} \end{cases}$$

and

$$H_\nabla(\mathbf{x}|) := \begin{cases} 1 & \text{if} \quad \mathbf{x} \in \nabla \\ 0 & \text{else} \end{cases} \ .$$

As with box spline we obtain half-box splines of higher order by successive convolutions,

$$H_\Delta(\mathbf{x}|\mathbf{v}_1 \dots \mathbf{v}_k) \ := \ \int_0^1 H_\Delta(\mathbf{x} - t\mathbf{v}_k|\mathbf{v}_1 \dots \mathbf{v}_{k-1})dt$$

and

$$H_\nabla(\mathbf{x}|\mathbf{v}_1 \dots \mathbf{v}_k) \ := \ \int_0^1 H_\nabla(\mathbf{x} - t\mathbf{v}_k|\mathbf{v}_1 \dots \mathbf{v}_{k-1})dt \ ,$$

where $k \ge 1$. Hence we assume that the directions are the unit directions,

$$\mathbf{v}_1, \dots, \mathbf{v}_k \in \{\mathbf{e}_1, \mathbf{e}_2, \mathbf{e}\} \ .$$

Note that the definitions of the two piecewise constant half-box splines $H_\Delta(\mathbf{x}|)$ and $H_\nabla(\mathbf{x}|)$ are not completely symmetric. Consequently any two half-box splines $H_\Delta(\mathbf{x}|\mathbf{v}_1 \dots \mathbf{v}_k)$ and $H_\nabla(\mathbf{x}|\mathbf{v}_1 \dots \mathbf{v}_k)$ sum to the box spline $B(\mathbf{x}|\mathbf{e}_1\mathbf{e}_2\mathbf{v}_1 \dots \mathbf{v}_k)$ even for $k = 0$. The two piecewise cubic C^1-half-box splines $H_\Delta(\mathbf{x}|\mathbf{e}_1\mathbf{e}_2\mathbf{e})$ and $H_\nabla(\mathbf{x}|\mathbf{e}_1\mathbf{e}_2\mathbf{e})$ are shown in Figure 17.

3.2. Basic Properties

As for box splines one can derive the following properties of half-box splines. Because of symmetry reasons it suffices to list these properties for $H(\mathbf{x}) := H_\Delta(\mathbf{x}|\mathbf{v}_1 \dots \mathbf{v}_k)$.

A half-box spline is **normalized** such that

$$\int_{\mathbb{R}^2} H(\mathbf{x})d\mathbf{x} = 1/2 \ .$$

Any k independent directions $\mathbf{u}_1, \dots, \mathbf{u}_k \in \mathbb{R}^k$ define a half-box $\vartheta := \{\sum \mathbf{u}_i\alpha_i \mid 0 \le \alpha_1 \le \alpha_2$ and $\alpha_2 \dots \alpha_k \in [0,1]\}$. The **density of the shadow** of this half-box represents a half-box spline. If π denotes the projection from $\mathbb{R}^k$ onto $\mathbb{R}^2$ mapping $\mathbf{u}_1, \dots, \mathbf{u}_k$ onto $\mathbf{v}_1, \dots, \mathbf{v}_k$, then

$$H(\mathbf{x}|\mathbf{v}_1 \dots \mathbf{v}_k) = \frac{1}{2\,\mathrm{vol}_k\vartheta} \mathrm{vol}_{k-2}(\pi^{-1}\mathbf{x} \cap \vartheta)$$

as illustrated in Figure 18.

From this geometric construction it follows that $H(\mathbf{x})$

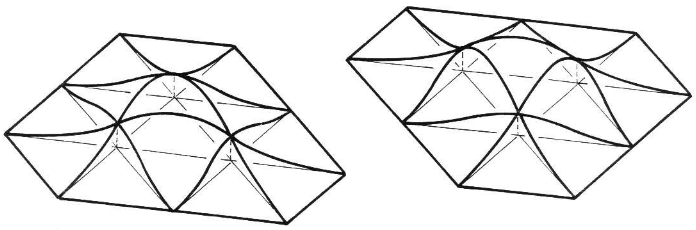

Figure 17. The two piecewise cubic C^1-half-box splines.

- *does not depend on the* **ordering** *of* $\mathbf{v}_3, \ldots, \mathbf{v}_k$,
- *is* **positive** *over the convex set* $\Delta + [\mathbf{v}_3 \ldots \mathbf{v}_k][0,1]^{k-2}$,
- *has the* **support** *closure*$(\Delta) + [\mathbf{v}_3 \ldots \mathbf{v}_k][0,1]^{k-2}$.

3.3. Derivatives and Polynomial Structure

The following further properties of half-box splines follow most easily from their inductive definition. The half-box spline $H(\mathbf{x})$

- *has the* **directional derivative**

$$D_{\mathbf{v}_r} H(\mathbf{x}) = H(\mathbf{x}|\mathbf{v}_3 \ldots \mathbf{v}_r^* \ldots \mathbf{v}_k) - H(\mathbf{x}-\mathbf{v}_r|\mathbf{v}_3 \ldots \mathbf{v}_r^* \ldots \mathbf{v}_k) \tag{10}$$

  with respect to $\mathbf{v}_r$, $r \geq 3$,

- *is* r *times* **continuously differentiable** *if all subsets of* $\{\mathbf{v}_1, \ldots, \mathbf{v}_k\}$ *obtained by deleting* $r+1$ *vectors* $\mathbf{v}_i$ *span* $\mathbb{R}^2$.
- *is polynomial of total degree* $\leq k-2$ *over all triangles* $\mathbf{i} + \Delta$ *and* $\mathbf{i} + \nabla, \mathbf{i} \in \mathbb{Z}^2$.

For example, the half-box splines $H_\Delta(\mathbf{x}|\mathbf{e}_1 \overset{k}{\ldots} \mathbf{e}_1\mathbf{e}_2 \overset{k}{\ldots} \mathbf{e}_2\mathbf{e}_3 \overset{k}{\ldots} \mathbf{e}_3)$ are $2k-1$ times continuous differentiable and are of polynomial degree $\leq 3k$.

4. Half-box Spline Surfaces

4.1. Translates of Half-Box Splines

Any pair of half-box splines

$$\begin{aligned} H_\Delta(\mathbf{x}) &:= H(\mathbf{x}|\mathbf{e}_3\mathbf{v}_1 \ldots \mathbf{v}_k) , \\ H_\nabla(\mathbf{x}) &:= H(\mathbf{x}|\mathbf{e}_3\mathbf{v}_1 \ldots \mathbf{v}_k) \end{aligned}$$

sums to the box spline $B(\mathbf{x}|\mathbf{e}_1\mathbf{e}_3\mathbf{v}_1 \ldots \mathbf{v}_k)$. Hence the translates $H_\Delta(\mathbf{x}-\mathbf{i})$ and $H_\nabla(\mathbf{x}-\mathbf{i})$, $\mathbf{i} \in \mathbb{Z}^2$, form a **partition of unity** .

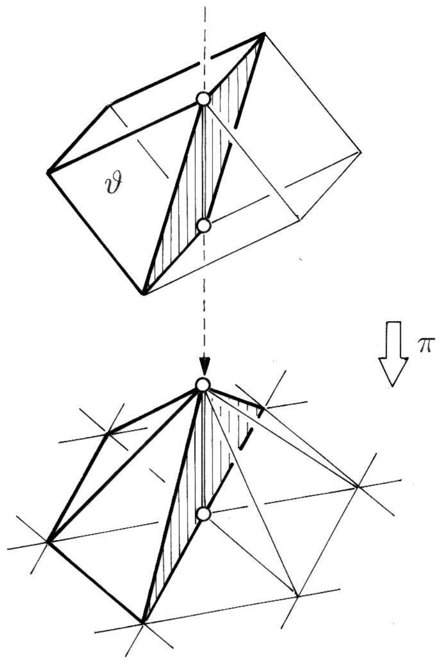

Figure 18. Geometric coonstruction of a half-box spline.

Consequently any **half-box spline surface**

$$\mathbf{s}(\mathbf{x}) = \sum_{\mathbf{i}\in\mathbb{Z}^2} (\mathbf{c}_{\mathbf{i}}^{\Delta} H_{\Delta}(\mathbf{x}-\mathbf{i}) + \mathbf{c}_{\mathbf{i}}^{\nabla} H_{\nabla}(\mathbf{x}-\mathbf{i}))$$

is an affine combination of its **control points** $\mathbf{c}_{\mathbf{i}}^{\Delta}$ and $\mathbf{c}_{\mathbf{i}}^{\nabla}$ and this representation is **affinely invariant** meaning that under any affine map the images of the control points control the image of $\mathbf{s}(\mathbf{x})$.

Since the half-box splines are non-negative, $\mathbf{s}(\mathbf{x})$ is even a convex combination of its control points and lies in their **convex hull**.

If we connect control points $\mathbf{c}_{\mathbf{i}}^{\Delta}$ and $\mathbf{c}_{\mathbf{j}}^{\nabla}$ whose associated triangles $\mathbf{i}+\Delta$ and $\mathbf{j}+\nabla$ have a common edge, then we obtain a hexagonal net, the control net of $\mathbf{s}$. An example is illustrated in Figure 19.

4.2. Derivatives and Polynomial Properties

The **directional derivative** of s with respect to $\mathbf{v}_r$ can be computed by the derivative formula (10) and it is

$$D_{\mathbf{v}_r}\mathbf{s}(\mathbf{x}) = \sum_{\mathbf{i}\in\mathbb{Z}^s} (\nabla_{\mathbf{v}_r}\mathbf{c}_{\mathbf{i}}^{\Delta} H_{\Delta}(\mathbf{x}|\mathbf{v}_1\ldots\mathbf{v}_r^*\ldots\mathbf{v}_k) + \nabla_{\mathbf{v}_r}\mathbf{c}_{\mathbf{i}}^{\nabla} H_{\nabla}(\mathbf{x}|\mathbf{v}_1\ldots\mathbf{v}_r^*\ldots\mathbf{v}_k)) ,$$

where $\nabla_{\mathbf{v}}\mathbf{c}_{\mathbf{i}} = \mathbf{c}_{\mathbf{i}} - \mathbf{c}_{\mathbf{i}-\mathbf{v}}$.

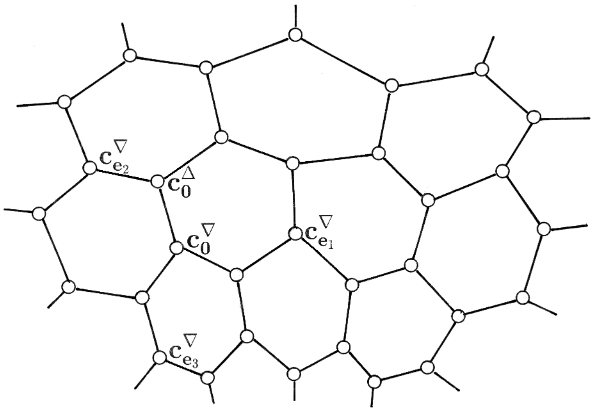

Figure 19. A hexagonal control net.

If $H_\Delta(\mathbf{x})$ is continuous or equivalently, if there are two independent directions among $\mathbf{v}_1, \ldots, \mathbf{v}_k$, then all directional derivatives of the sum of all shifts, $\sum H_\Delta(\mathbf{x}-\mathbf{i})$, are zero. Therefore this sum is a constant function. Because of symmetry reasons and since the shifts of both half-box splines H_Δ and H_∇ form a partition of unity, we get

$$\sum_{\mathbf{i}\in\mathbb{Z}^2} H_\Delta(\mathbf{x}-\mathbf{i}) = \sum_{\mathbf{i}\in\mathbb{Z}^2} H_\nabla(\mathbf{x}-\mathbf{i}) = 1/2 \ . \tag{11}$$

In particular, this implies that the shifts of H_Δ and H_∇ are **linearly dependent** .

Further, if the box spline $B(\mathbf{x}) = B(\mathbf{x}|\mathbf{e}_1\mathbf{e}_2\mathbf{v}_1\ldots\mathbf{v}_k) = H_\Delta(\mathbf{x}) + H_\nabla(\mathbf{x})$ is continuous, we recall from (6) in 2.2 that

$$\sum_{\mathbf{i}\in\mathbb{Z}^2} \mathbf{m_i}(H_\Delta(\mathbf{x}-\mathbf{i}) + H_\nabla(\mathbf{x}-\mathbf{i})) = \mathbf{x} \ ,$$

where $\mathbf{m_i}$ is the center of supp$B(\mathbf{x}-\mathbf{i})$. If H_Δ is continuous, we can use (11) and get for any $\mathbf{v}\in\mathbb{R}^2$

$$\sum_{\mathbf{i}\in\mathbb{Z}^2}((\mathbf{m_i}+\mathbf{v})H_\Delta(\mathbf{x}-\mathbf{i}) + (\mathbf{m_i}-\mathbf{v})H_\nabla(\mathbf{x}-\mathbf{i})) = \mathbf{x} \ .$$

For example, if $\mathbf{v} = (\mathbf{e}_1-\mathbf{e}_2)/6$, then the points $\mathbf{m_i^\Delta} := \mathbf{m_i}+\mathbf{v}$ and $\mathbf{m_i^\nabla} := \mathbf{m_i}-\mathbf{v}$ form a regular hexagonal grid as illustrated in Figure 20.

Since the half-box spline representation is affinely invariant, we obtain for any linear polynomial $l(\mathbf{x})$

$$l(\mathbf{x}) = \sum_{\mathbf{i}\in\mathbb{Z}^2}(l(\mathbf{m_i^\Delta})H_\Delta(\mathbf{x}-\mathbf{i}) + l(\mathbf{m_i^\nabla})H_\nabla(\mathbf{x}-\mathbf{i})) \ .$$

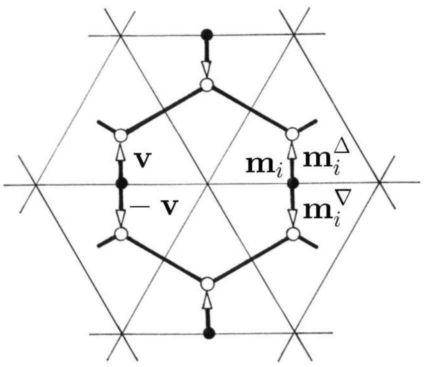

Figure 20. The hexagonal grid of the "centers" $\mathbf{m}_{\mathbf{i}}^{\Delta}$ and $\mathbf{m}_{\mathbf{i}}^{\nabla}$.

This property is referred to as the **linear precision** of the half-box spline representation.

4.3. Subdivision

Any half-box spline surface

$$s(\mathbf{x}) = \sum_{\mathbf{i} \in \mathbb{Z}^2} (\mathbf{c}_{\mathbf{i}}^{\Delta} H_{\Delta}(\mathbf{x} - \mathbf{i}) + \mathbf{c}_{\mathbf{i}}^{\nabla} H_{\nabla}(\mathbf{x} - \mathbf{i}))$$

has also a "finer" representation

$$s(\mathbf{x}) = \sum_{\mathbf{i} \in \mathbb{Z}^2} (\mathbf{d}_{\mathbf{i}}^{\Delta} H_{\Delta}(m\mathbf{x} - \mathbf{i}) + \mathbf{d}_{\mathbf{i}}^{\nabla} H_{\nabla}(m\mathbf{x} - \mathbf{i}))$$

for any $m \in \mathbb{N}$.

As for box splines one can derive a subdivision algorithm for the computation of the new control points $\mathbf{d}_k^{\square}(\mathbf{i}) = \mathbf{d}^{\square}(\mathbf{i})$ from the control points $\mathbf{c}_{\mathbf{i}}^{\diamond}$, where $\square$ and $\diamond \in \{\Delta, \nabla\}$. This algorithm which is due to [28] is given by the recursion

$$\begin{aligned} \mathbf{d}_r^{\square}(\mathbf{i}) &:= \frac{1}{m} \sum_{l=0}^{m-1} \mathbf{d}_{r-1}^{\square}(\mathbf{i} - l\mathbf{v}_r) \ , \quad r = 3, \ldots, k \ . \\ \mathbf{d}_2^{\square}(\mathbf{i}) &:= \mathbf{c}_{\mathbf{j}}^{\diamond} \end{aligned}$$

for $\mathbf{i}, \mathbf{j} \in \mathbb{Z}^2$ and $\mathrm{supp} H^{\square}(m\mathbf{x} - \mathbf{i}|) \subset \mathrm{supp} H^{\square}(\mathbf{x} - \mathbf{j}|)$.

One can also combine the recursion steps. For example for $m = 2$ and for the symmetric cubic half-box splines, where $\mathbf{v}_3 \ldots \mathbf{v}_k = \mathbf{e}_1\mathbf{e}_2\mathbf{e}_3$ the $\mathbf{d}_5^{\square}(\mathbf{i})$ can be computed from the $\mathbf{c}_{\mathbf{i}}^{\diamond}$ by the masks shown in Figure 21 and from the $\mathbf{d}_2^{\diamond}(\mathbf{i})$ by the mask shown in Figure 22.

As with box splines the control points $\mathbf{d}^{\square}(\mathbf{i})$ converge to the half-box spline surface $\mathbf{s}$ with order $O(1/m^2)$.

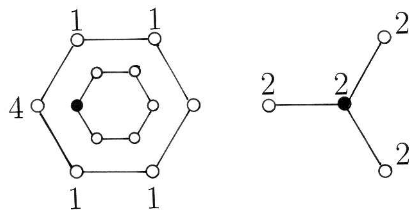

Figure 21. The masks to subdivide cubic C^1-half-box spline surfaces.

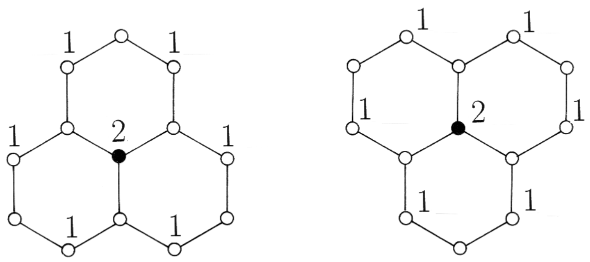

Figure 22. The mask for three averaging steps.

4.4. Bézier Representation

One can compute the Bézier points of a half-box spline surface by the same recursion as for box spline surfaces [35,1,28]. The only difference is that the recursion terminates differently. For example if, e.g., $\mathbf{v}_1\mathbf{v}_2\mathbf{v}_3 = \mathbf{e}_1\mathbf{e}_2\mathbf{e}_3$, then

$$\mathbf{b}_3 = \alpha_3 * C_3\mathbf{b}_0 \ ,$$

where

$$C_3\mathbf{b}_0(\mathbf{j}) = \begin{cases} \mathbf{c}_\mathbf{i}^\Delta & \text{if} \quad \mathbf{j} = 3\mathbf{i} + \mathbf{e}_1 - \mathbf{e}_3 \\ \mathbf{c}_\mathbf{i}^\nabla & \text{if} \quad \mathbf{j} = 3\mathbf{i} + \mathbf{e}_2 - \mathbf{e}_3 \\ \mathbf{0} & \text{otherwise} \end{cases} .$$

This means that the Bézier points $\mathbf{b}_3(\mathbf{i})$ of a piecewise cubic C^1-half-box spline can be computed from the hexagonal control net $\mathbf{c}$ with the masks shown in Figure 23.

4.5. Generalized Half-Box Spline Surfaces

As with box splines it is possible to build arbitrary free form surfaces with the half-box splines

$$H_\Delta^k(\mathbf{x}) := H_\Delta(\mathbf{x}|\mathbf{e}_1\mathbf{e}_2\mathbf{e}_3 \overset{k}{\ldots} \mathbf{e}_1\mathbf{e}_2\mathbf{e}_3) \quad \text{and} \quad H_\nabla^k(\mathbf{x}) := H_\nabla(\mathbf{x}|\mathbf{e}_1\mathbf{e}_2\mathbf{e}_3 \overset{k}{\ldots} \mathbf{e}_1\mathbf{e}_2\mathbf{e}_3) \ ,$$

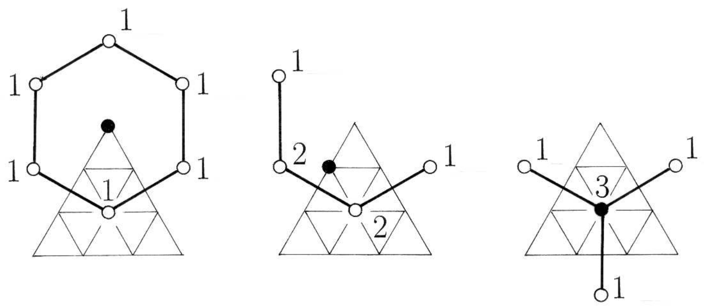

Figure 23. The masks for the Bézier points of the cubic half-box splines.

see [38,33]. The support of a half-box spline $H^k_\Delta(\mathbf{x})$ consists of k rings of triangles around a triangle as shown in Figure 24 for $k = 1, 2$. This implies that any triangular patch of a half-box spline surface

$$\mathbf{s}(\mathbf{x}) = \sum_{\mathbf{i} \in \mathbb{Z}^2} (\mathbf{c}_\mathbf{i}^\Delta H^k_\Delta(\mathbf{x}) + \mathbf{c}_\mathbf{i}^\nabla H^k_\nabla(\mathbf{x}))$$

is controlled by k rings of control points around a single control point as illustrated schematically in Figure 25 for $k = 1, 2$.

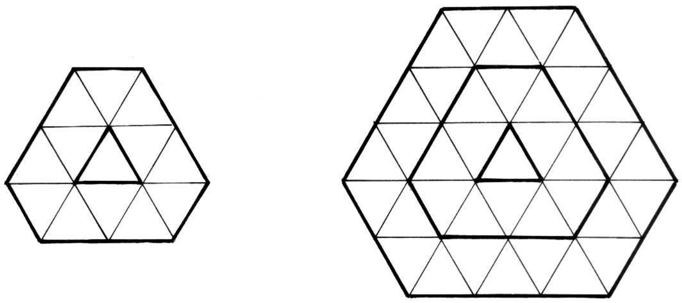

Figure 24. Support of the half-box splines H^2_Δ (left) and H^3_Δ (right).

We will call the net controlling one triangular patch a **minimal net** or a **H-primitive** of order k. Note that the H-primitives of order k are dual to the B-primitives of order $k+1$. This means that the triangles and interior vertices of the dual B-primitive correspond to the vertices and hexagonal meshes of the H-primitive.

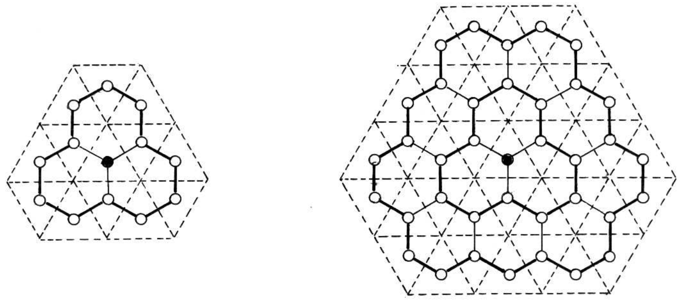

Figure 25. H-primitives of order 2 (left) and 3 (right).

A **generalized half-box spline surface** of order k is given by an arbitrary control net with isolated non-hexagonal meshes and consists of all triangular patches controlled by a H-primitive of order k that is part of the entire control net.

For any generalized half-box spline surface $\mathbf{s}_H$ of order k there is a generalized box spline surface $\mathbf{s}_B$ of order $k+1$ whose control net is dual to the control net of the generalized half-box spline surface. Hence $\mathbf{s}_H$ and $\mathbf{s}_B$ have the same number of triangular patches and these have the same topological adjacencies.

In particular, this is true for nets with multiple control points. Consequently, if $k-1$ rings of control points around an m-sided mesh coalesce, then the corresponding half-box spline surface has a hole whose boundary is given by m triangular patches.

Figure 26 shows a generalized half-box spline surface (middle) of order $k=1$ with its control net (left) and with a G^1-filling (right).

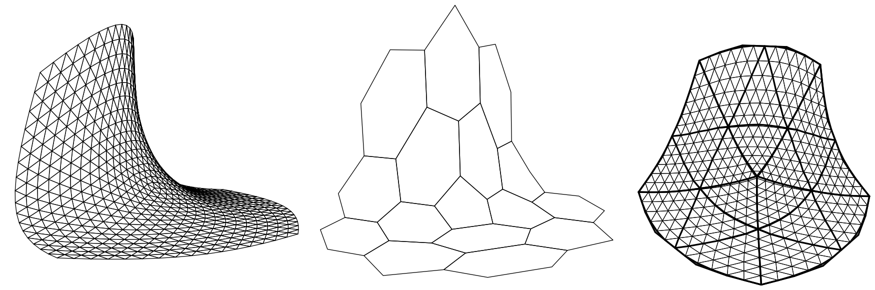

Figure 26. A generalized half box spline surface with smooth filling (left), control net (middle) and Bézier net (right). (courtesy of Markus Florenz and Georg Umlauf)

REFERENCES

1. W. Boehm (1983). Generating the Bézier points of triangular splines, in Surfaces in Computer Aided Geometric Design, R.E. Barnhill and W. Boehm (eds.), Elsevier Science Publishers B.V. (North-Holland), 77-91.
2. W. Boehm (1983). The de Boor algorithm for triangular splines, in Surfaces in Computer Aided Geometric Design, R.E. Barnhill and W. Boehm (eds.), Elsevier Science Publishers B.V. (North-Holland), 109-120.
3. W. Boehm1983. Subdividing multivariate splines. Computer Aided Design 15, 345-352.
4. W. Boehm (1984). Calculating with box splines. Computer Aided Geometric Design, 1, 149-162.
5. W. Boehm, H. Prautzsch and P. Arner (1987). On triangular splines. Constr. Approx,3, 157-167.
6. C. de Boor, R. DeVore 1983. pproximation by smooth multivariate splines, Trans. Amer. Math. Soc. 276, 775-788.
7. C. de Boor (1993). On the evaluation of box splines. Numer. Algorithms 5, 5-23.
8. C. de Boor and Höllig (1982). Recurrence relations for multivariate B-splines. Proc. Amer. Math. Soc., 85, 397-400.
9. C. de Boor and Höllig (1982). B-splines from parallelepipeds. J. Analyse Math., 42, 99-115.
10. C. de Boor, K. Höllig and S. Riemenschneider (1993). Box splines. Springer.
11. G. M. Chaikin1974.An algorithm for high speed curve generation. Computer Graphics and Image Processing 3, 346-349.
12. E. Cohen, T. Lyche and R. Riesenfeld (1984). Discrete Box splines and refinement algorithms. Comput. Aided Geom. Design, 1, 131-148
13. M. Dæhlen (1989). On the evaluation of Box-splines. in Mathematical Methods in Computer Aided Geometric Design, T. Lyche and L. Schumaker (eds.), Academic Press, N.Y., 167-179
14. W. Dahmen (1986). Subdivision algorithms converge quadratically. J. Comput. Appl. Math., 16, 145-158
15. W. Dahmen, N. Dyn and D. Levin (1985). On the convergence rates of subdivision algorithms for box spline surfaces. Constr. Approx., 1, 305-322
16. W. Dahmen and C. A. Micchelli (1983). Translates of multivariate splines. Linear Algebra Appl., 52, 217-234
17. W. Dahmen and C. A. Micchelli (1984). Subdivision algorithms for the generation of box-spline surfaces. Comput. Aided Geom. Design, 1, 115-129.
18. W. Dahmen and C. A. Micchelli (1985). Line average algorithm: a method for the computer generation of smooth surfaces. Comput. Aided Geom. Design, 2, 77-85.
19. W. Dahmen and C. A. Micchelli (1985). On the local linear independence of translates of a box spline. Studia Math., 82, 243-262.
20. W. Dahmen and C. A. Micchelli (1988). Convexity of multivariate Bernstein polynomials and box spline surfaces. Studia Math., 23, 265-287.
21. P. O. Frederickson (1970). Triangular spline interpolation. Rpt.6 70, Lakehead Univ.
22. P. O. Frederickson (1971). Generalized triangular splines. Rpt.7 71, Lakehead Univ.

23. Rong-qing Jia (1984). Linear independence of translates of a box spline. J. Approx. Theory, 40, 158-160.
24. Rong-qing Jia (1985). Local linear indepence of the translates of a box spline. Constr. approx., 1, 175-182.
25. L. Kobbelt (1997). Stable Evaluation of Box Splines Numerical Algorithms 14 (1997) 4, pp. 377–382.
26. J. M. Lane and R. F. Riesenfeld1980. A theoretical development for the computer generation and display of piecewise polynomial surfaces. IEEE Trans. Pattern Anal. Mach. Intellig. 2, 35-45.
27. C.T. Loop1987. Smooth subdivision surfaces based on triangles. Master's thesis, University of Utah.
28. H. Prautzsch (1984). Unterteilungsalgorithmen für multivariate Splines - ein geometrischer Zugang. Dissertation, Univ. Braunschweig.
29. H. Prautzsch (1985). Generalized subdivision and convergence. Comput. Aided Geom. Design, 2, 69-75.
30. H. Prautzsch (1986). The location of the control points in the case of box splines. IMA J. Numer. Anal., 6, 43-49.
31. H. Prautzsch 1992. On convex Bézier triangles. Mathematical Modelling and Numerical Analysis 26, 23-36.
32. H. Prautzsch 1997. Freeform splines. Computer Aided Geometric Design 14, 201-206.
33. H. Prautzsch and G. Umlauf. Triangular G^2 splines, in Laurent et.al. (eds) Curves and Surface Design, Vanderbilt University Press (1999) 335-342.
34. G. de Rham (1947). Un peu de mathematique à propos d'une courbe plane, Elem. Math. 2, 73-76,89-97.
35. M. A. Sabin (1977). The use of piecewise forms for the numerical representation of shape. Dissertation, MTA Budapest.
36. I.J. Schoenberg (1946). Contributions to the problem of approximation of equidistant data by analytic functions, Part A: On the problem of smoothing of graduation, a first class of analytic approximation, Quart. Appl Math. 4, 45-99.
37. A. Sommerfeld (1904). Eine besondere anschauliche Ableitung des Gaussischen Fehlergesetzes, in Festschrift Ludwig Boltzmann gewidmet zum 60. Geburtstage, Verlag von J.A. Barth, Leipzig, 848-859.
38. G. Umlauf (1999). Glatte Freiformflächen und optimierte Unterteilungsflächen. Dissertation, Univ. Karlsruhe.

Index